Investigating potential use of SNF for district heating

Lorenzo Mazzocco

January 2020

Contents

Abstract

Spent nuclear fuel (SNF) is often thought of as the main waste from the traditional means of electricity and heat production by nuclear fission and it's mostly perceived as a liability instead of a simple byproduct or even a useful commodity. In reality spent nuclear fuel has the unique characteristic of spontaniously generating power through nuclear decay of the unstable isotopes generated after the irradiation of virgin or recycled fuel. In a carbon costrained world would therefore be a severe missed opportunity not to take advantage of this autonomous source of power as a mean of energy generation. Thus we will investigate the potential use of already discharged spent nuclear fuel assemblies as a heat source for district heating applications characterizing the thermodynamic and radiologic constrains that are to be addressed in order to engineer the above mentioned system.

Part I

Characterization of spent nuclear fuel

Chapter 1

Decay heat production assessment

In order to use nuclear fuel in a nuclear reactor newly produced fuel pellets are stacked on top of each other inside a neutron-trasparent cladding made from steel and zirconium alloys forming a fuel rod. Then multiple cladded fuel rods are arranged in a fixed structure hold together by a strong steel and zircaloy grid-like support pieces forming a fuel assembly[1].There is considerable variation among fuel assemblies designed for the different types of reactor.
In this chapter we are interested in obtaining a rough estimation of the decay heat power produced by SNF evolution in time for different types of assemblies and for different burn up times. We will base our future calculations on a 2011 simulation by Oak Ridge National Laboratory (ORNL) [2] and a 2006 study by SBK comprehensive of direct calorimetric measurements of SNF assemblies [3].

1.1 ORNL Simulation

The simulation is based on the ORNL developed software SCALE [4] and concerns both PWR and BWR spent nuclear fuel assemblies geometries. UOX and MOX (RG: reactor grade, WG: weapon grade) fuel pellets are compared for 4 different burn up points at discharge (35, 40, 45, and 50 GWd/MTHM).

The following geometries are used for the simulation:

Table 1.1 - PWR 17×17 Westinghouse fuel bundle[5] specifics

Pitch [cm]	21.403
Height* [cm]	385.140
Height** [cm]	405.892
Heavy metal mass [kg]	ca. 460

Table 1.2 - BWR 7x7 General Electric fuel bundle[5] specifics

Pitch [cm]	15.240
Height* [cm]	365.760
Height** [cm]	434.656
Heavy metal mass [kg]	ca. 200

The results for the decay heat power production densities are reported in the following tables and figures:

*: active fuel assembly height. **: total assembly height (comprehensive of top and bottom nozzles).

Table 1.3 - Decay heat densities for PWR and BWR UOX fuel bundles at 35 and 50 GWd/MTHM for selected times after discharge [kW/MTHM]

Time after discharge (days)	PWR		BWR	
	35	50	35	50
10	53.2	78.0	52.8	77.6
100	18.5	27.9	18.2	27.4
900	3.4	5.6	3.3	5.4
9300	0.85	1.3	0.8	1.2

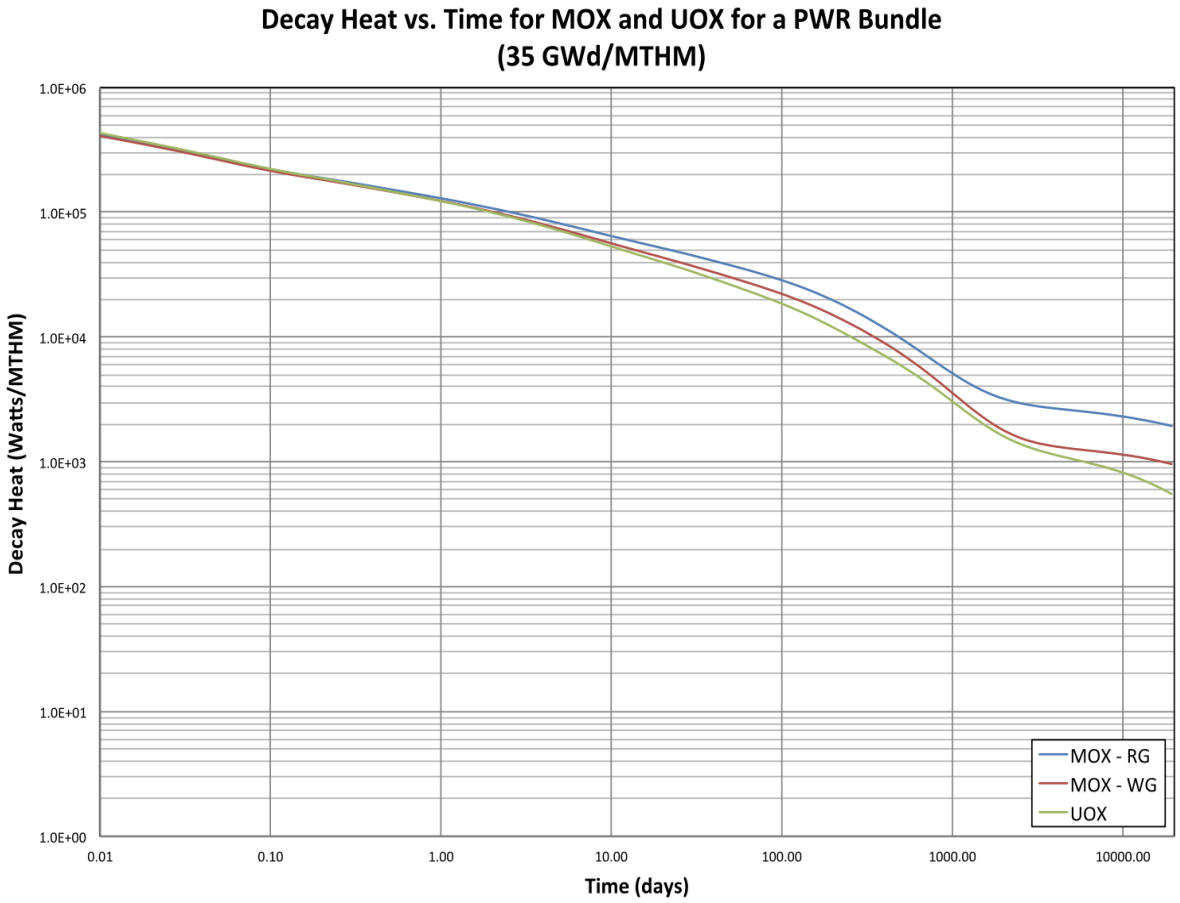

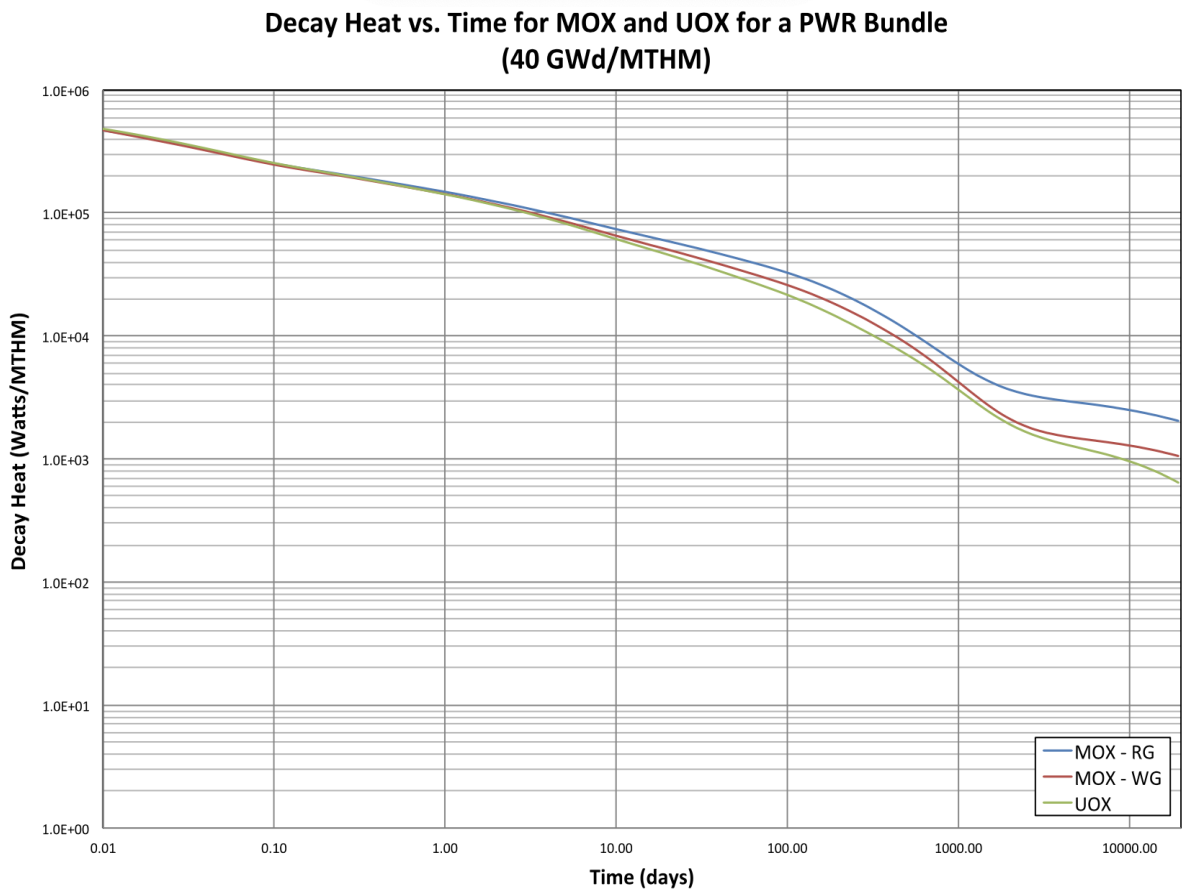
Decay Heat vs. Time for MOX and UOX for a PWR Bundle
(40 GWd/MTHM)
Decay Heat (Watts/MTHM)
1.0E+06
1.0E+05
1.0E+04
1.0E+03
1.0E+02
1.0E+01
1.0E+00
0.01
0.10
1.00
10.00
100.00
1000.00
10000.00
Time (days)
MOX - RG
MOX - WG
UOX

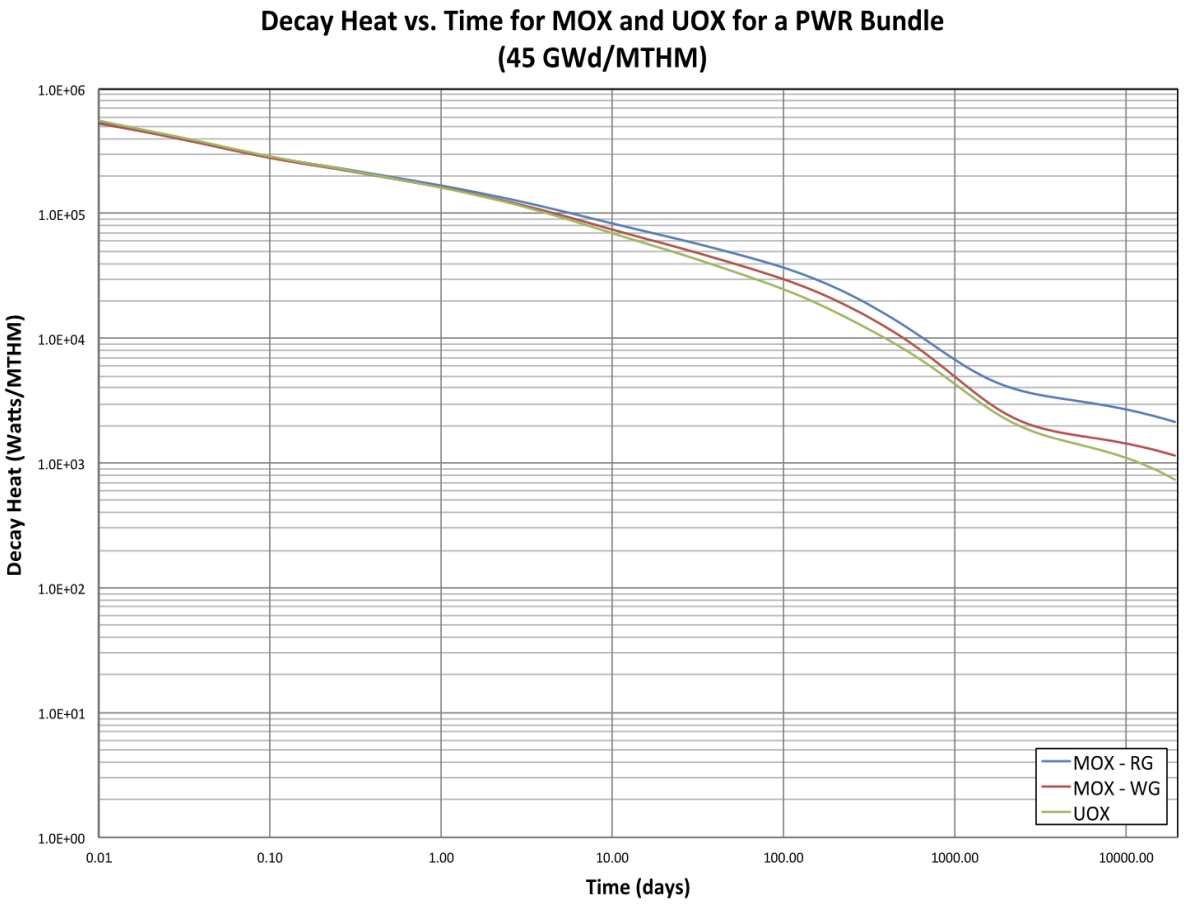
Decay Heat vs. Time for MOX and UOX for a PWR Bundle
(45 GWd/MTHM)
Decay Heat (Watts/MTHM)
1.0E+06
1.0E+05
1.0E+04
1.0E+03
1.0E+02
1.0E+01
1.0E+00
0.01
0.10
1.00
10.00
100.00
1000.00
10000.00
Time (days)
MOX - RG
MOX - WG
UOX

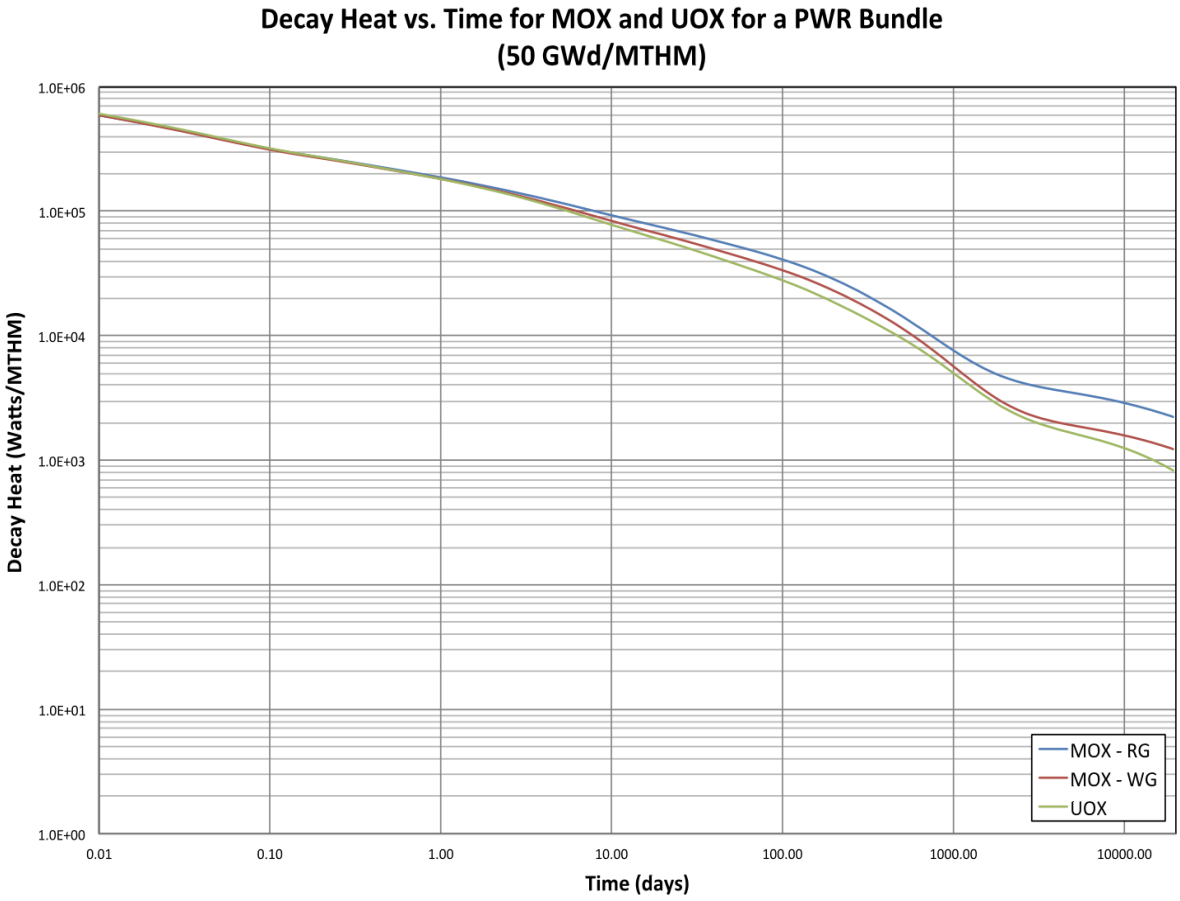
Decay Heat vs. Time for MOX and UOX for a PWR Bundle
(50 GWd/MTHM)
Decay Heat (Watts/MTHM)
1.0E+06
1.0E+05
1.0E+04
1.0E+03
1.0E+02
1.0E+01
1.0E+00
0.01
0.10
1.00
10.00
100.00
1000.00
10000.00
Time (days)
MOX - RG
MOX - WG
UOX

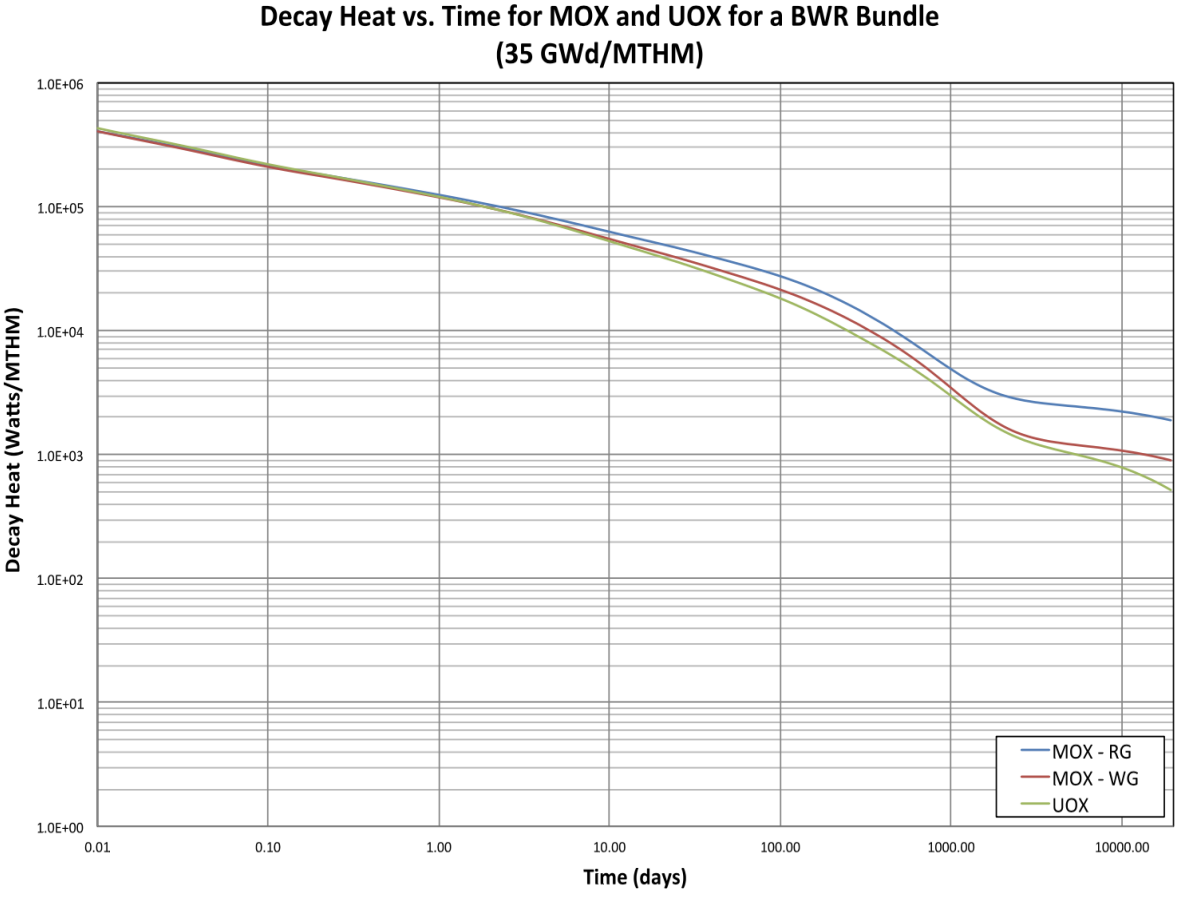
Decay Heat vs. Time for MOX and UOX for a BWR Bundle
(35 GWd/MTHM)
Decay Heat (Watts/MTHM)
1.0E+06
1.0E+05
1.0E+04
1.0E+03
1.0E+02
1.0E+01
1.0E+00
0.01
0.10
1.00
10.00
100.00
1000.00
10000.00
Time (days)
MOX - RG
MOX - WG
UOX

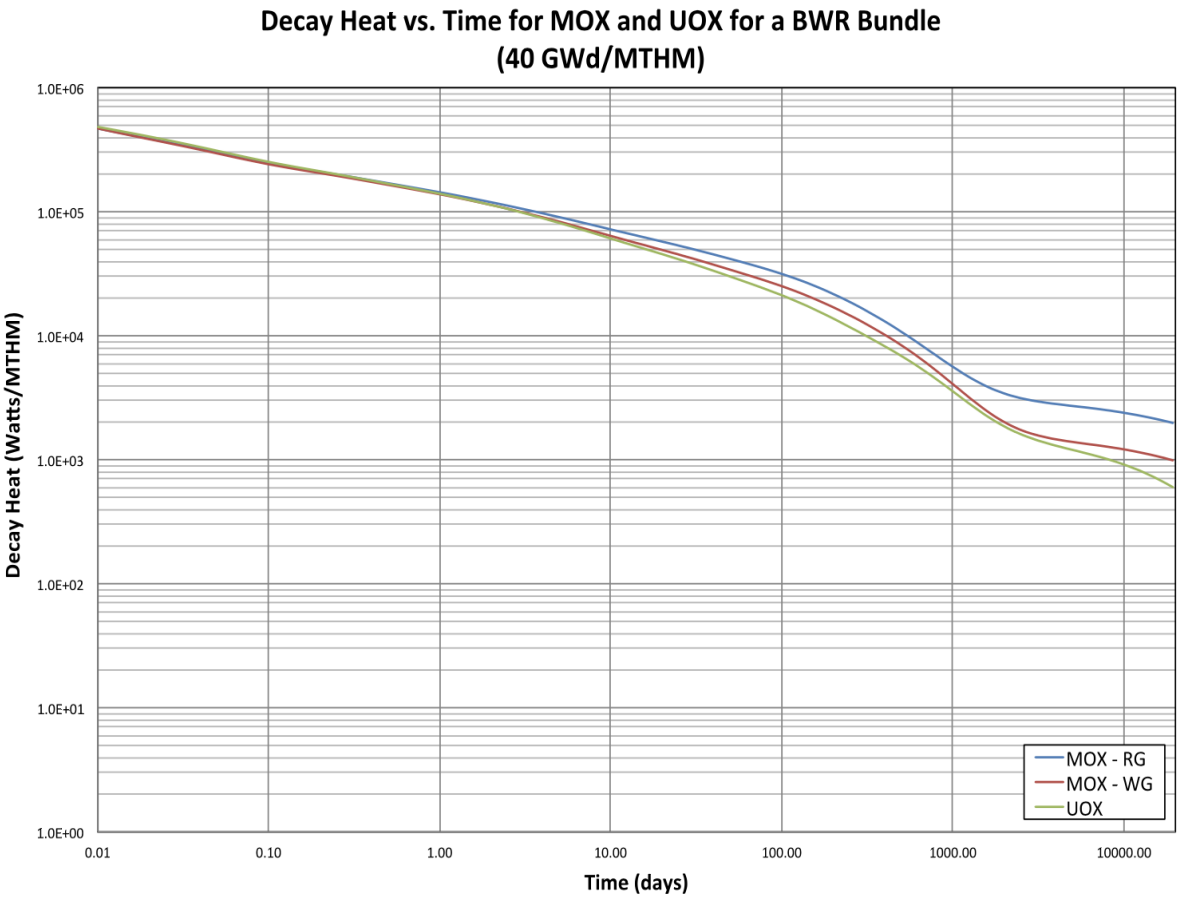
Decay Heat vs. Time for MOX and UOX for a BWR Bundle
(40 GWd/MTHM)
Decay Heat (Watts/MTHM)
1.0E+06
1.0E+05
1.0E+04
1.0E+03
1.0E+02
1.0E+01
1.0E+00
0.01
0.10
1.00
10.00
100.00
1000.00
10000.00
Time (days)
MOX - RG
MOX - WG
UOX

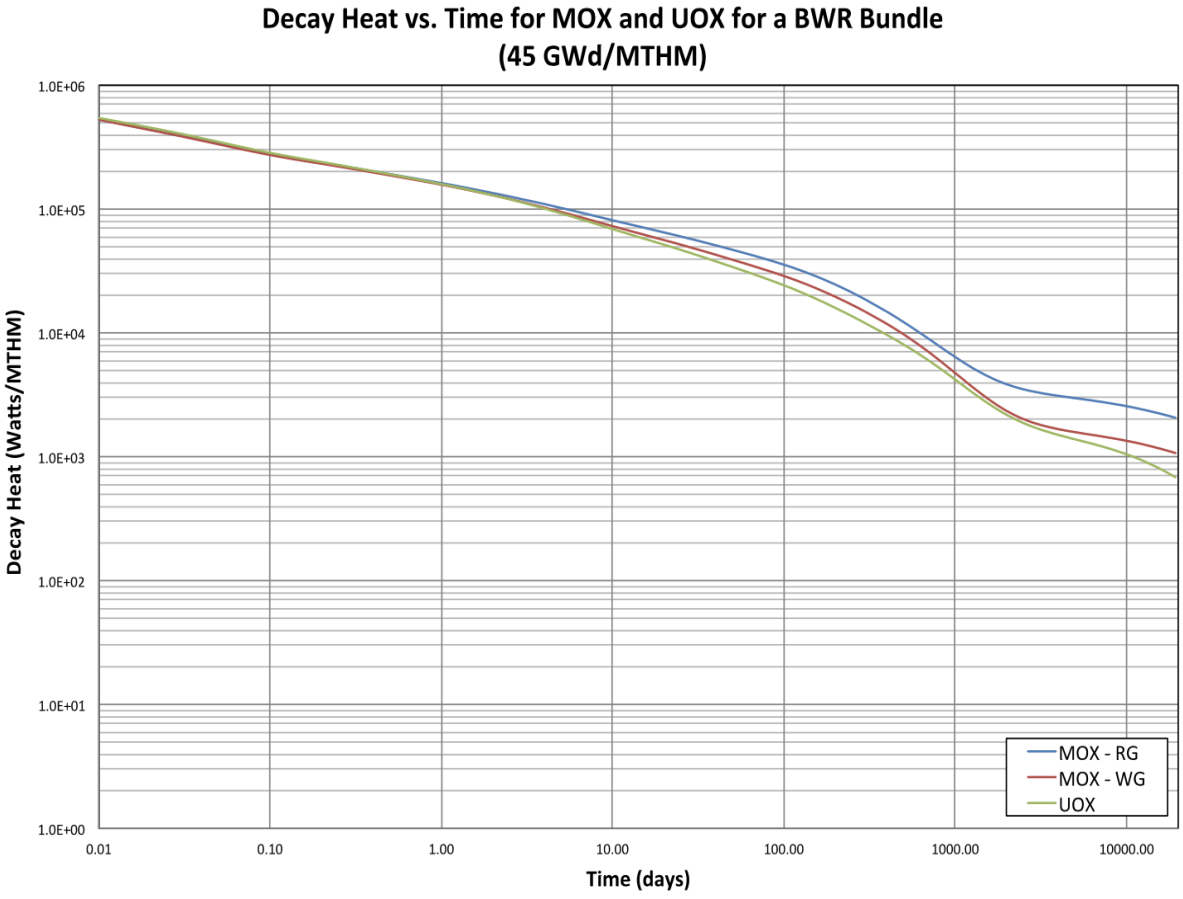
Decay Heat vs. Time for MOX and UOX for a BWR Bundle
(45 GWd/MTHM)
Decay Heat (Watts/MTHM)
1.0E+06
1.0E+05
1.0E+04
1.0E+03
1.0E+02
1.0E+01
1.0E+00
0.01
0.10
1.00
10.00
100.00
1000.00
10000.00
Time (days)
MOX - RG
MOX - WG
UOX

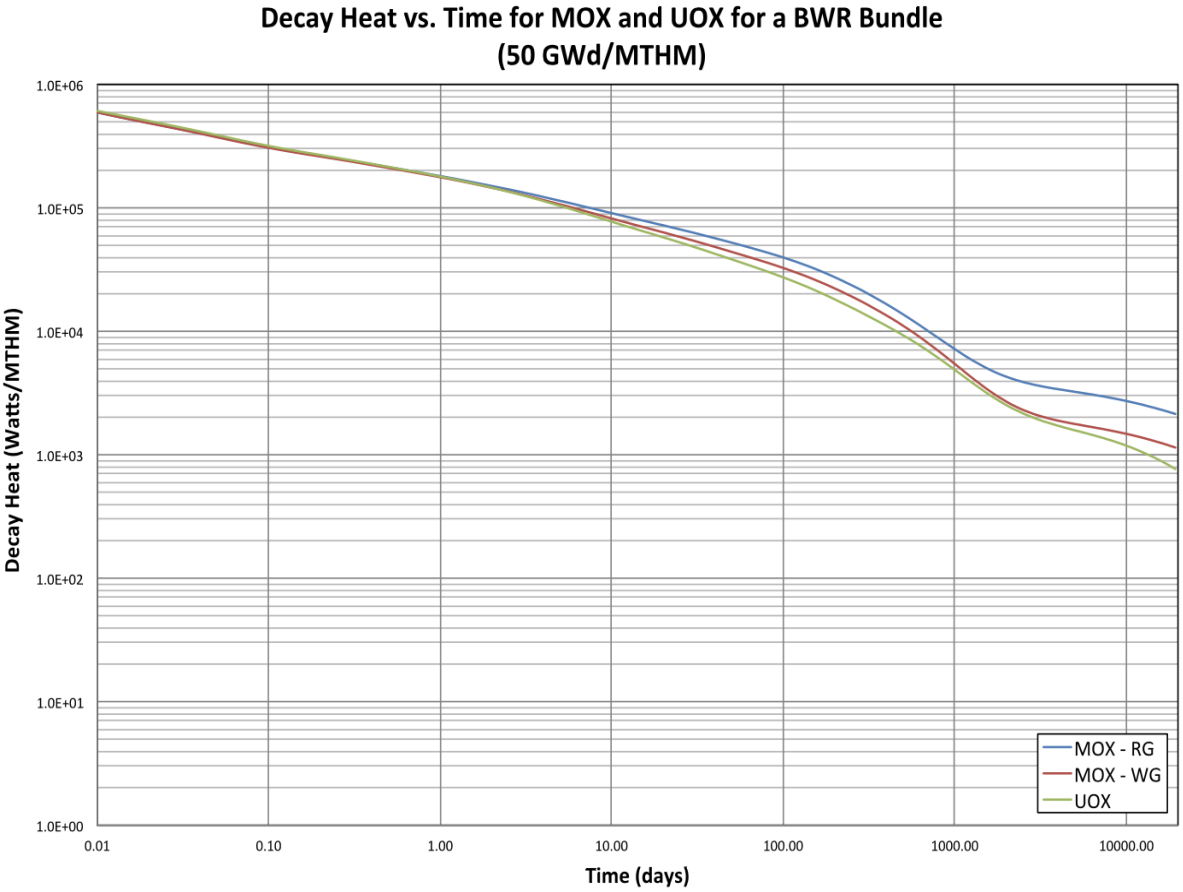

1.2 SKB Data and SCALE code validation

The study consists of 109 calorimetric measurements of decay heat from a set of PWR and BWR assemblies from the SKB's Clab inventory.

50 BWR and 34 PWR assemblies were selected for measurement from the Clab inventory. The selected assemblies met the following criteria:

- Fuel types PWR: 15×15, 17×17 and BWR: 8×8, Svea64, Svea100 were included.
- Assemblies were gamma scanned in this measurement campaign and fuel has long cooling times.
- The assemblies possessed a large spread in burnup.
- The assemblies possessed a large spread in initial enrichment.
- The assemblies possessed long cooling times.
- The assemblies did not contain inserts as boron glass rods, neutron sources or other parts.
- The assemblies were not mechanically damaged or had leaking rods

The decay heat loss caused by gamma radiation leakage from the calorimetric apparatus is calculated and added to the measured value. The experiment shows consistent results with the ORNL simulations for the assemblies of interest. We can therefore consider the data obtained by the SCALE simulation valid for subsequent calculations.

*: volume is computed including assembly nozzles. **: volume is computed excluding assembly nozzles.

1.3 Discussion

Knowing the heavy metal content and volume for each assembly tipe we can elaborate on the data obtained by ORNL to compute **power produced per assembly (kW/Assembly)** and **volumetric power densities (kW/m³)**. From here on end we are going to consider only UOX fuel bundles.

From tables 1.1 and 1.2 we can compute the total volume of each bundle tipe.

Table 1.4 - PWR 17×17 Westinghouse fuel bundle[5] specifics

Total volume* [m^3]	0.18593
Active fuel volume** [m^3]	0.17643
Heavy metal mass [MTHM]	0.46

Table 1.5 - BWR 7x7 General Electric fuel bundle[5] specifics

Volume* [m^3]	0.10095
Active fuel volume** [m^3]	0.08495
Heavy metal mass [MTHM]	0.20

The following tables are computed using total assembly volume.

Table 1.6 - Decay heat densities for PWR and BWR UOX fuel bundles at 35 and 50 GWd/MTHM for selected times after discharge [kW/MTHM]

Time (days)	Time (years)	PWR		BWR	
		35	50	35	50
10	0.0	53.230	78.030	52.820	77.350
100	0.3	18.520	27.930	18.240	27.400
200	0.5	11.950	18.570	11.700	18.150
300	0.8	8.866	14.050	8.658	13.710
500	1.4	5.912	9.543	5.767	9.308
1100	3.0	2.766	4.549	2.698	4.427
1500	4.1	2.032	3.343	1.983	3.245
2100	5.8	1.548	2.517	1.511	2.437
2500	6.8	1.391	2.240	1.358	2.166
3100	8.5	1.253	1.994	1.223	1.925
3300	9.0	1.221	1.937	1.192	1.868
3800	10.4	1.158	1.824	1.130	1.758
5300	14.5	1.038	1.613	1.009	1.549
6300	17.3	0.981	1.516	0.952	1.453
7300	20.0	0.932	1.435	0.902	1.371
8300	22.7	0.887	1.361	0.857	1.298
9300	25.5	0.847	1.295	0.815	1.231
10300	28.2	0.808	1.233	0.776	1.170
11300	31.0	0.773	1.175	0.740	1.112
12300	33.7	0.739	1.121	0.706	1.058
14300	39.2	0.679	1.024	0.644	0.961
15300	41.9	0.650	0.979	0.616	0.917
16300	44.7	0.624	0.938	0.589	0.876
17300	47.4	0.5986	0.8989	0.5642	0.8375

Table 1.7 - Decay heat per assembly for PWR and BWR UOX fuel bundles at 35 and 50 GWd/MTHM for selected times after discharge [kW/Assembly]

Time (days)	Time (years)	PWR		BWR	
		35	**50**	**35**	**50**
10	0.0	24.486	35.894	10.564	15.470
100	0.3	8.519	12.848	3.648	5.480
200	0.5	5.497	8.542	2.340	3.630
300	0.8	4.078	6.463	1.732	2.742
500	1.4	2.720	4.390	1.153	1.862
1100	3.0	1.272	2.093	0.540	0.885
1500	4.1	0.935	1.538	0.397	0.649
2100	5.8	0.712	1.158	0.302	0.487
2500	6.8	0.640	1.030	0.272	0.433
3100	8.5	0.576	0.917	0.245	0.385
3300	9.0	0.562	0.891	0.238	0.374
3800	10.4	0.533	0.839	0.226	0.352
5300	14.5	0.477	0.742	0.202	0.310
6300	17.3	0.451	0.697	0.190	0.291
7300	20.0	0.429	0.660	0.180	0.274
8300	22.7	0.408	0.626	0.171	0.260
9300	25.5	0.390	0.596	0.163	0.246
10300	28.2	0.372	0.567	0.155	0.234
11300	31.0	0.356	0.541	0.148	0.222
12300	33.7	0.340	0.516	0.141	0.212
14300	39.2	0.312	0.471	0.129	0.192
15300	41.9	0.299	0.450	0.123	0.183
16300	44.7	0.287	0.431	0.118	0.175
17300	47.4	0.275	0.413	0.113	0.168

Table 1.8 - Decay heat volumetric densities for PWR and BWR UOX fuel bundles at 35 and 50 GWd/MTHM for selected times after discharge [kW/m^3]

Time (days)	Time (years)	PWR		BWR	
		35	**50**	**35**	**50**
10	0.0	131.691	193.045	104.644	153.241
100	0.3	45.818	69.099	36.136	54.283
200	0.5	29.564	45.942	23.179	35.958
300	0.8	21.934	34.760	17.153	27.161
500	1.4	14.626	23.609	11.425	18.440
1100	3.0	6.843	11.254	5.345	8.770
1500	4.1	5.027	8.271	3.929	6.429
2100	5.8	3.830	6.227	2.993	4.828

2500	6.8	3.441	5.542	2.690	4.291
3100	8.5	3.100	4.933	2.423	3.814
3300	9.0	3.021	4.792	2.362	3.701
3800	10.4	2.865	4.513	2.239	3.483
5300	14.5	2.568	3.991	1.999	3.069
6300	17.3	2.427	3.751	1.885	2.879
7300	20.0	2.306	3.550	1.786	2.716
8300	22.7	2.194	3.367	1.697	2.572
9300	25.5	2.095	3.204	1.614	2.439
10300	28.2	1.999	3.050	1.538	2.318
11300	31.0	1.912	2.907	1.466	2.203
12300	33.7	1.828	2.773	1.399	2.096
14300	39.2	1.680	2.533	1.276	1.904
15300	41.9	1.608	2.422	1.220	1.817
16300	44.7	1.544	2.321	1.167	1.736
17300	47.4	1.481	2.224	1.118	1.659

It is clear that the examined fuel bundles produce considerable power through nuclear decay. In particular during the first year the power densities for all burnup times stick to values greater than 15 kW/m^3. Then they decrease incrementally slower staying in the 1 - 5 kW/m^3 range even after 40 years since discharge.
Let's consider the number of assemblies (PWR 17x17) and volumes necessary to obtain a cumulative 10 MWt of power in function of time since discharge:

Table 1.9 - Number of PWR 17x17, 35 GWd/MTHM assemblies and volume occupied to obtain 10 MWt of cumulative power

Time [years]	Power [kW/m^3]	Power [kW/Assembly]	Volume [m^3]	N. Assemblies
31.00	1.91	0.36	5229.05	28123
20.00	2.31	0.43	4336.97	23325
9.00	3.02	0.56	3310.44	17804
3.00	6.84	1.27	1461.34	7859

Table 1.10 - Number of PWR 17x17, 50 GWd/MTHM assemblies and volume occupied to obtain 10 MWt of cumulative power

Time [years]	Power [kW/m^3]	Power [kW/Assembly]	Volume [m^3]	N. Assemblies
31.00	2.91	0.54	3439.97	18484
20.00	3.55	0.66	2816.90	15152
9.00	4.79	0.89	2086.76	11223
3.00	11.25	2.09	888.57	4778

From tables 1.9 and 1.10 we realize that the most important factor influencing the feasibility of a heat producing power system is the time elapsed since discharge. In order to reach 10 MWt (potential nominal power of a medium-sized waste-to-energy plant) cumulative power and keep the number of PWR assemblies below the 10.000 threshold it is necessary to employ a distribution of fuel bundles with less than 8 years of lifetime for high-burnup assemblies or less then 4 years for low-burnup assemblies.

Chapter 2

Radiological assessment

We are concerned with performing a radiological assessment of SNF bundles for multiple reasons. First of all we are interested with the isotopic composition of the irradiated fuel in order to identify potentially dangerous radioisotopes to account for during the design phase of our system (i.e. volatile fission products), secondly we are concerned with radiation-induced damages to surrounding structures and components and finally we want to characterize the overall radiation enviroment around the assemblies to predict possible interaction with the coolant (i.e. neutron activation).

2.1 Radionuclide inventory

DA FARE

Fare simulazione ORIGEN.

2.2 Neutron production

There are two mechanisms that result in a net production of neutrons in light water reactor SNF: spontaneous fission of specific radioisotopes and (α, n) reactions. The resulting neutron flux is a function of assembly size and geometry and most importantly burnup time. Highly irradiated fuel rods produce more radiation and in particular more neutrons since the quantity of unstable isotopes generated is greater than low burnup fuel rods.

2.2.1 Spontaneous fission

During the initial period of decay (first years after discharge) spontaneous fission accounts for around 80% of the total neutron production. The following tables show the major isotopes responsible for neutron production by fission per MTHM for both PWR/BWR assemblies for different burnups (medium and high) computed using the ORIGEN2 code by the US Department of Energy [6]:

Table 2.1 - Variation in neutron production (neutrons/s*MTHM) by spontaneous fission as a function of time since discharge for a 40 GWd/MTHM BWR assembly type

Isotopes	Time since discharge [yrs]		
	1	**10**	**100**
U-238	-	-	1.19E+04
Pu-238	6.29E+05	5.98E+05	2.94E+05
Pu-240	2.25E+06	2.26E+06	2.26E+06
Pu-242	1.04E+06	1.04E+06	1.04E+06
Cm-242	1.04E+08	7.11E+04	4.70E+04
Cm-244	5.15E+08	3.65E+08	1.16E+07
Cm-246	2.58E+06	2.58E+06	2.55E+06
Cm-248	-	-	8.58E+03
TOTAL	**6.25E+08**	**3.72E+08**	**1.78E+07**

Table 2.2 - Variation in neutron production (neutrons/s*MTHM) by spontaneous fission as a function of time since discharge for a 60 GWd/MTHM PWR assembly type

Isotopes	Time since discharge [yrs]		
	1	**10**	**100**
U-238	-	-	1.16E+04
Pu-238	-	-	6.18E+05
Pu-240	2.71E+06	2.76E+06	2.85E+06
Pu-242	2.00E+06	2.00E+06	2.00E+06
Cm-242	1.79E+08	9.11E+04	6.02E+04
Cm-244	2.14E+09	1.51E+09	4.83E+07
Cm-246	2.11E+07	2.11E+07	2.08E+07
Cm-248	-	-	1.62E+05
Cf-252	9.45E+06	8.88E+05	-
TOTAL	**2.35+09**	**1.54E+09**	**7.48E+07**

From the data it is clear that during the first 10 years after discharge the majority of neutrons come from the curium isotopes ^{244}Cm and ^{242}Cm.

2.2.2 (α, n) reactions

A significan part of neutron production by (α, n) reactions comes from ^{17}O(α, n)^{20}Ne and ^{18}O(α, n)^{21}Ne (interaction with UO_2) [7]. The following tables show the major isotopes responsible for neutron production by (α, n) reaction per MTHM for both PWR/BWR assemblies for different burnups (medium and high) computed using the ORIGEN2 code by the US Department of Energy [6]:

Table 2.3 - Variation in neutron production (neutrons/s*MTHM) by (α, n) reactions as a function of time since discharge for a 40 GWd/MTHM BWR assembly type

Isotopes	Time since discharge [yrs]		
	1	**10**	**100**
Pu-238	3.86E+06	3.67E+06	1.80E+06
Pu-239	2.23E+05	2.23E+05	2.22E+05
Pu-240	4.26E+05	4.28E+05	4.30E+05
Am-241	4.19E+05	1.94E+06	4.18E+06
Am-243	2.42E+04	2.41E+04	2.39E+04
Cm-242	2.15E+07	1.46E+04	9.69E+03
Cm-243	4.84E+04	3.89E+04	4.36E+03
Cm-244	4.28E+06	3.03E+06	9.68E+04
TOTAL	**3.08E+07**	**9.37E+06**	**6.77E+06**

Table 2.4 - Variation in neutron production (neutrons/s*MTHM) by (α, n) reactions as a function of time since discharge for a 60 GWd/MTHM PWR assembly type

Isotopes	Time since discharge [yrs]		
	1	**10**	**100**
Pu-238	8.14E+06	7.71E+06	3.79E+06
Pu-239	2.67E+05	2.67E+05	2.67E+05
Pu-240	5.14E+05	5.23E+05	5.40E+05
Am-241	5.53E+05	2.65E+06	5.73E+06
Am-243	6.16E+04	6.15E+04	6.10E+04
Cm-242	3.69E+07	1.88E+04	1.24E+04
Cm-243	1.22E+05	9.77E+04	1.10E+04
Cm-244	1.77E+07	1.26E+07	4.01E+05
TOTAL	**6.43E+07**	**2.39E+07**	**1.08E+07**

As for the neutron production by spontaneous fission the major contributors are curium isotopes, specifically ^{244}Cm and ^{242}Cm.

2.2.3 Total neutron production

We have analyzed in detail the sources of the neutron flux and identified the same major contributors for both mechanisms (^{244}Cm and ^{242}Cm). With the half-life of ^{242}Cm being 160 days it quickly decades leaving ^{244}Cm as the single biggest neutron source after 10 years. The following table considers the contribution for the two mechanism to compute the total production for the assemblies considered in the previuos sections:

Table 2.5 - Total neutron production (neutrons/s*MTHM) as a function of time since discharge for a 40 GWd/MTHM BWR assembly type

Isotopes	Time since discharge [yrs]		
	1	10	100
Cm-242	1.26E+08	8.57E+04	5.67E+04
Cm-244	5.19E+08	3.68E+08	1.17E+07
TOTAL	**6.45E+08**	**3.68E+08**	**1.18E+07**

Table 2.6 - Total neutron production (neutrons/s*MTHM) as a function of time since discharge for a 60 GWd/MTHM PWR assembly type

Isotopes	Time since discharge [yrs]		
	1	10	100
Cm-242	2.16E+08	1.10E+05	7.26E+04
Cm-244	2.16E+09	1.52E+09	4.87E+07
TOTAL	**2.37E+09**	**1.52E+09**	**4.88E+07**

From the results we understand that the most important variable is burnup time and since the neutronic enviroment in the reactor and the fuel enrichment is very similar there is little difference between PWR and BWR spent fuel assemblies. The following chart is taken from a 2020 study [8] assessing the neutron activation of structural materials in SNF dry casks storage systems, it represents the neutron emission rate from one 16x16 PWR 55 GWd/MTHM assembly:

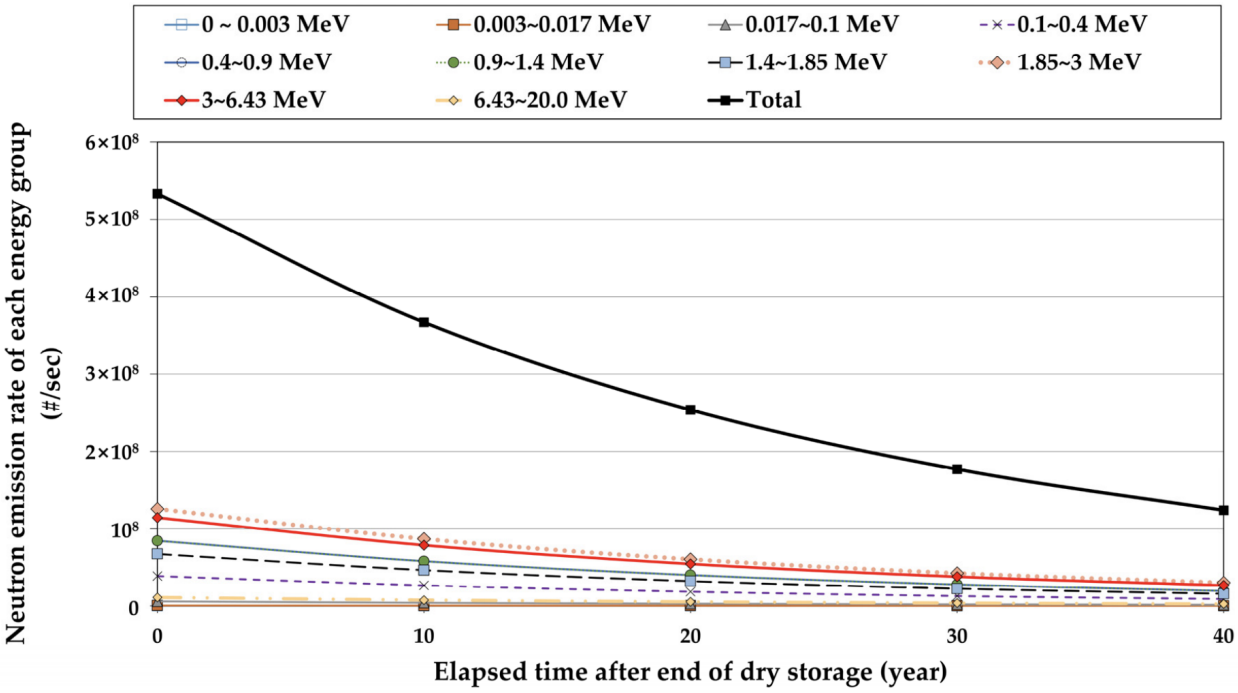

Figure 2.1 - Neutron emission rate for different energy groups from a 16x16 PWR 55 GWd/MTHM assembly as a function of time *(Time starts at end of wet storage, 10 years after reactor discharge). [8]

The results seem to confirm the computation elaborated by the DOE, the majority of the neutrons are characterized by an energy of 1.4-6.43 MeV. The neutron emission rate curve tends to follow a decay with half-life of around 19 years which is explained by the relative importance of the different isotopes contributing (the half-life of ^{244}Cm is 18.1 yrs).

2.3 Gamma radiation production

After discharge there is a great number of radioactive isotopes emitting gamma radiation, because of this the energy spectrum of the photons emitted is quite large. The following tables show the production of photons divided into different energy groups for a 40 GWd/MTHM BRW and a 60 GWd/MTHM PWR assembly type as a function of time since discharge (only photons with an energy > 1 MeV are shown):

Table 2.7 - Variation in photons production (photons/s*MTHM) as a function of time since discharge for a 40 GWd/MTHM BWR assembly type [6]

Mean Energy	**Time since discharge [yrs]**		
[MeV]	**1**	**10**	**100**
1.3	1.06E+15	2.00E+14	5.87E+11
1.8	6.70E+13	4.11E+12	4.14E+10
2.3	9.85E+13	5.42E+10	8.17E+06
2.8	1.89E+12	4.26E+09	2.32E+08
3.5	2.37E+11	5.24E+08	1.96E+06
5.0	2.79E+07	1.64E+07	8.33E+05
7.0	3.12E+06	1.89E+06	9.54E+04
9.5	3.69E+05	2.17E+05	1.09E+04
TOTAL	**1.23E+15**	**2.04E+14**	**6.29E+11**

Table 2.8 - Variation in photons production (photons/s*MTHM) as a function of time since discharge for a 60 GWd/MTHM PWR assembly type [6]

Mean Energy	**Time since discharge [yrs]**		
[MeV]	**1**	**10**	**100**
1.3	2.28E+15	4.70E+14	8.49E+11
1.8	1.15E+14	7.21E+12	5.85E+10
2.3	1.42E+14	8.42E+10	2.09E+07
2.8	3.16E+12	7.76E+09	6.47E+08
3.5	3.99E+11	9.77E+08	7.72E+06
5.0	1.04E+08	6.76E+07	3.30E+06
7.0	1.20E+07	7.80E+06	3.79E+05
9.5	1.37E+06	8.96E+05	4.35E+04
TOTAL	**2.54E+15**	**4.77E+14**	**9.08E+11**

The large majority of gamma radiation comes from the decay of fission products (they make 99% of total production at 10 years since discharge and drop to about 90% after 100 years since discharge). Contributions from actinides and their daughters and activation products are negligible during the first years after discharge.

Part II

Fuel safety criteria

This part of the study is a review of the existing nuclear fuel safety criteria and regulations adopted by the nuclear industry and main nuclear countries around the world. Given the characteristics of our engineering problem we are not interested in the safety criteria as they relate to normal operating conditions, anticipated operating occurrences (AOOs) or accident conditions (such as LOCA or RIA) of a light water reactor but rather as they relate to the enviroment our particular system is going to generate. From this point of view it is far more useful to base our considerations on medium term fuel dry storage best practices and regulations. Therefore we are going to perform an in depth assessment of dry storage technologies, normal operation conditions and fuel degradation processes affecting features of these systems, only subsequently we will recall the regulatory limits for fuel safety (e.g. maximum fuel pellet temperature, maximum cladding temperature, etc.) operating in an active LWR reactor environment. Since every country relies on his domestic nuclear regulator for specific legislation we will base our review on the US Nuclear Regulatory Commission's (US NRC or NRC) standards on the topic in order to study the regulatory framework. The assessment of the fuel performance, the safety boundaries and present regulations is a fundamental step that will help us design the best system given the problem requirements and the fuel limitations.

Chapter 3

Dry Storage Systems Safety Criteria

Dry-storage systems are regulated by the US NRC in accordance with 10 CFR 72 [9] and NUREG-1536 and very precise and useful information is given by the ISG-11 Rev.3 [10].

The storage process begins with the loading of the fuel bundles in the cask happening inside the plant cooling pool. Then the water and moisture are removed from the cask and the system is backfilled with an inert gas (helium, nitrogen or other). Finally the cask is permanently bolted and welded.
Heat generated by the SNF in a loaded system is transported from the assemblies to the basket structure by convection of the inert gas, conduction where the assemblies touch the basket structure, and radiation. Heat then moves from the basket structure to the inner cask or canister wall by the same mechanisms. Metal cask bodies typically have external heat transfer fins and are cooled by air flow past the fins. The fins are required for casks containing fairly recent SNF to meet the temperature limit requirements of the used fuel. Canisters within concrete casks are cooled by natural convection of air introduced from air inlets at the bottom of the concrete. In heat from the hot canister wall warms air entering via inlets and gives it buoyant force, inducing a natural air circulation upward and out of the upper exhaust vents in a self-sustained manner.[11]

3.1 Normal operation conditions

The major concerns for safety during normal operations in a dry storage systems are cladding temperature, canister pressure over time and chemical enviroment over time.

3.1.1 Cladding temperature history

The NRC Spent Fuel Project Office Interim Staff Guidance - 11 [10] addresses the technical review aspects of and specifies the acceptance criteria for limiting spent fuel reconfiguration in storage casks. The guidance states that in order to assure integrity of the cladding material, the following criteria should be met:

1. For all fuel burnups (low and high), the maximum calculated fuel cladding temperature should not exceed 400 °C for normal conditions of storage and short-term loading operations (e.g., drying, backfilling with inert gas, and transfer of the cask to the storage pad). However, for low burnup fuel, a higher short-term temperature limit

may be used, if the applicant can show by calculation that the best estimate cladding hoop stress is equal to or less than 90 MPa the temperature limit proposed.

2. During loading operations, repeated thermal cycling (repeated heatup/cooldown cycles) may occur but should be limited to less than 10 cycles, with cladding temperature variations that are less than 65°C each.

3. For off-normal and accident conditions, the maximum cladding temperature should not exceed 570°C.

It is however specified that all the casks designed before issuance of ISG-11 Rev. 2 were certified with a short-term cladding temperature limit applicable to fuel loading operations of 570 °C in contrast to the current value of 400°C. In the report the guidance [10] states that:

"*Given the conservatism used in calculating peak clad temperatures for low burnup fuel, the staff has reasonable assurance that storage cask systems which use the 570°C temperature limit for low burnup fuel loading operations will continue to perform as expected when the casks were originally certified. Therefore, there is no need to require the licensees of storage-only or dualpurpose cask systems to repackage spent fuel that was loaded using the 570°C temperature limit.*"

The Electric Power Research Institute (EPRI) performed various thermal simulations regarding dry storage systems [12]. The cladding temperature history for the hottest axial position of the fuel rod is computed for a 40-year dry storage period, the figure shows the mathematical fit to the computed temperatures given the 400°C peak cladding temperature (PCT) limit at loading prescribed by the ISG-11 Rev.2 in °K:

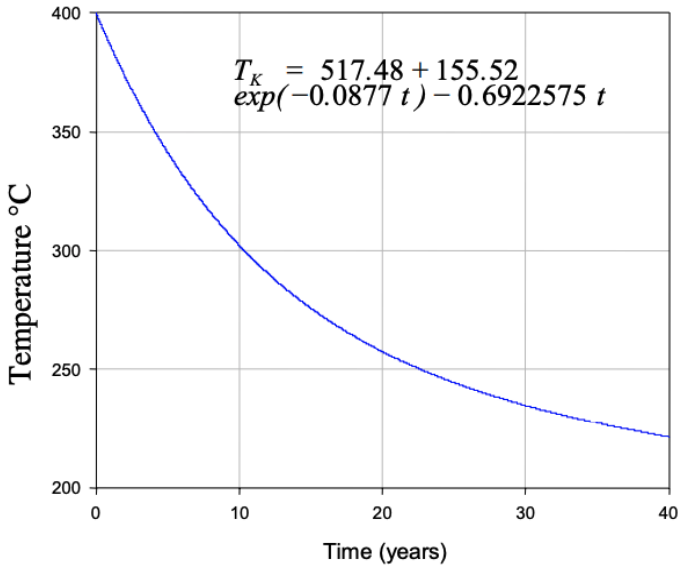

Figure 2.1 - Cladding Temperature History for High-Burnup Spent Fuel in Dry Storage Casks [12]

The cladding temperature can therefore potentially remain higher than 300°C for an initial period of 10 years since fuel loading. The same report summarizes the effect of such temperatures on two of the main cladding damage mechanisms dependent on temperature

* active and passive degradation processes of cladding are scrutinized in-depth in a subsequent section.

(stress corrosion cracking (SCC) and delayed hydride cracking (DHC)) stating that the dry storage enviroment (including the cladding temperature history summarized in figure 2.1) is not conducive to the initiation of either mechanism[12][13]*.

Various studies confirm the validity of the NRC threshold of 400/570°C for peak cladding temperature [14][15] and even other nuclear regulators like the UK's Office for Nuclear Regulations [16] accepts these values. However other investigations indicate more conservative PCT values to be preferrable such as 250°C - 300°C [17] or <250°C [18]. The Japan nuclear regulator (NRA) requires the peak cladding temperature to be less than 250°C and 275°C depending on fuel burnup [19].

3.1.2 Canister pressure

The pressure of the inert gas inside a dry cask storage system over time depends on inital backfill pressure, evolution of the assemblies' temperature profile, the amount of free water in vapor form, release of fission products in a gaseous form and other mechanisms. Initial backfill helium pressure for different dry cask storage systems recently licenced by the NRC are given below:

Table 3.1 - Minimum and maximum backfill helium pressure for different dry cask storage systems licensed by NRC [20][21][22][23]

Company	Model	Min Pressure [atm]	Max Pressure [atm]
TN Americas LLC	NUHOMSA® EOS	0.10	0.24
TN Americas LLC	Advanced NUHOMSA®-24PT1	0.00	0.20
TN Americas LLC	Advanced NUHOMSA®-24PT4	0.41	0.48
TN Americas LLC	NUHOMSA®-HD-32PTH	1.10	1.24
TN Americas LLC	TN-68	1.80	2.00
NAC International, Inc.	NAC-MPC	1.02	1.16

Simulating the pressure evolution throught time and assuming only mechanisms that increase pressure "such calculations yield values of up to 0.35 MPa (50.8 psi) internal pressurization of commercial fuel container from hydrated uranium oxides [assuming 1 kg of UO3·2H2O which yields 112 g of water] heated to 250°C by decay heat after sealing."[24]. This value related to the design of dry cask storage systems and the conditions of irradiated fuel rods at the time of loading should not be sufficient to damage the system and should therefore be considered negligible.

3.1.3 Chemical enviroment

The chemical enviroment inside the canister includes the backfill inert gas, residual water, potentially fission products and galvanization products. The main concern is the removal of water present in the canister at the moment of fuel loading via repeated depressurizations and backfillings of helium inside the system. Inside the canister we can find bound (liquid or vapor) or unbound water. An evaluation study commissioned by the NRC reports that the total residual water present in the system is estimated to amount between 5 and 55 moles (equivalent to 0.1 L to 1.0 L of liquid water at 25°C, 1atm) [25].

3.2 Active degradation processes affecting fuel

We are concerned only with degradation processes that affect fuel in the short and mid term since the long term effects would not act in a meaningful way on the fuel in our hypothetical system.

3.2.1 Fuel-pellet oxidation

Fuel pellets are made of uranium dioxide (UO_2) in a ceramic form. UO_2 is thermodinamically unstable in air (or other oxidizing atmosphere) and will eventually oxidize to U_3O_8 wich exists only in as a powder. The oxidation of UO2 to U3O8 is a function of the time at temperature, initial grain size, burnup, and oxygen availability but of those temperature is the most critical parameter [26]. It has been shown that the oxidation process will occur by first oxidizing the cubic phase UO_2 to a cubic phase denoted by U_4O_{9+x} or $UO_{2.4}$ (type 1 oxidation) and then finally from $UO_{2.4}$ to U_3O_8 (type 2 oxidation). The most important difference between type 1 and 2 oxidation is that during the first a volumetric contraction of the fuel pellet takes place [27] and during the latter the reduced density of the U_3O_8 powder will bring a 31 to 36 percent increase in volume (bulking)[27] inducing great mechanical stress on the cladding. The following tables list the time for (nominal) type 1 and 2 oxidation as a function of temperature (type 1,2) and burnup (type 2) for fuel pellets exposed to air:

Table 3.2 - Time for complete type 1 oxidation of SNF, from UO_2 to $UO_{2.4}$, as a function of temperature [28]

Temperature [°C]	**Time [yrs]**	**Time [days]**
100	809	2.95 E+06
150	1.48	540
200	0.63	230
250	0.049	18
300	0.006	2

Table 3.3 - Time for complete type 2 oxidation of SNF, from $UO_{2.4}$ to U_3O_8, as a function of temperature and burnup [28]

Burnup [GWd/MTHM]	**20**	**30**	**50**
Temperature [°C]	**Time [yrs]**	**Time [yrs]**	**Time [yrs]**
100	3.5 E+06	8.9 E+07	5.6 E+10
150	5440	9300	2.8 E+07
200	33	417	68000
250	0.5	5	522
300	0.02	0.14	9

It is clear from tables 3.2 and 3.3 that the inert atmosphere is crucial in order to avoid quick oxidation at medium to high temperatures and subsequent cladding stress. It is also interesting to note that high burnup fuel tends to perform type 2 oxidization at a much

slower paste than low burnup fuel; given the upward trend of fuel irradiation time in recent years we can state that the risk of cladding stress due to fuel oxidation and subsequent polverization will be negligible for a loss of inert atmosphere accident due to the relatively short time repressurize the system with an adequate gas.

3.2.2 Cladding tangential creep rupture

Creep is the progressive deformation of a material under stress. In dry storage conditions the stresses are created by a difference of pressure between the inside of the cladding and the outside atmosphere. In particular during the vacuum drying operations the pressure difference is at a maximum and the other important factor, temperature, is high aswell. Experimental creep results have shown that Zircaloy cladding retains sufficient ductility if kept below 400°C. To ensure the mechanical integrity of the cladding material, the following criteria should be met: (1) for all fuel burnups, the maximum calculated fuel-cladding temperature for normal operations of drying, transfer (short-term loading), and storage should not exceed 400°C; and (2) for short-term off-normal and accident conditions, the maximum cladding temperature should not exceed 570°C. [11]

3.2.3 Cladding stress corrosion cracking (SCC)

During the activity inside the reactor the thermo-mechanical interaction of fuel pellets with the inner surface of the cladding creates incipient cracks on the latter [29][30]. Stress corrosion cracking involves both chemical corrosion and mechanical stress and generates growth of the cracks created on the inner surface; in particular the mechanism depends on volatile-fission-product chemistry and large tensile hoop stresses. It is found that the major contributor to chemical corrosion in SCC between fission products is iodine with a treshold concentration of $5 \cdot 10^{-6}$ g/cm^2 in order to initiate the process [31]. Below 400°C pure thermal diffusion is the only mechanism active to release new iodine gas, but at this temperature there is essentially no release of iodine without cracking of fuel pellets or other extraordinary fragmentation mechanisms.

3.2.4 Cladding hydrogen-related mechanisms

A consequence of in-reactor activity is a phenomenon called pickup, the absorption of part of the hydrogen produced by corrosion mechanisms in the Zircaloy metal by diffusion. When the hydrogen exceeds the solubility limit in the cladding it precipitates with zirconium forming zirconium hydrides.
Hydrogen concentration and temperature gradients in the cladding cause a migration of the hydrides called redistribution. Another important mechanism is hydride reorientation which involves the dissolving of pre-existing circumferentially oriented hydrides and then the re-precipitation of zirconium hydrides oriented perpendicular to the hoop stress (radial hydrides). High burnup fuels are more susceptible to hydride precipitation and the related phenomena of hydride reorientation during vacuum drying. The main phenomena caused by precipitation of zirconium hydrides are hydrogen embrittlement and delayed hydride cracking (DHC):

Hydrogen embrittlement. The embrittlement of the cladding is caused when the hydride content is large enough to cause deleterious effects on mechanical properties of the metal (e.g. tensile ductility, fracture toughness). This mechanism is caused by decreasing temperatures and tightly depends on the orientation of the hydride deposits with radial hydrides being the necessary element to cause embrittlement [11].

Delayed Hydride cracking. The following text is extracted directly from a 2013 Southwest Research Institute review [33]. "In DHC, hydrogen in the cladding diffuses to a region of high tensile stress where it deposits as hydrides in a direction normal to the tensile stresses. Under suitable conditions, the hydrides may fracture and result in an incremental extension of the crack tip. After crack extension, the extended crack tip becomes dormant for a period of time until sufficient amounts of hydrogen have diffused to the crack-tip region and precipitated as hydrides. Then the cracking process repeats itself and results in the intermittent crack growth phenomenon called DHC. [...] In general, DHC velocity decreases rapidly with decreasing temperatures because the diffusion of hydrogen to the crack tip is slow at low temperatures". The dependence of DHC velocity on temperature is complex and we can differentiate two regions divided by a treshold temperature above which the physics of the relationship change drastically[32][33]. This treshold is around 318°C. Below 318°C cracking velocity is directly proportional on temperature. Above 318°C the DHC velocity "decreases abruptly with increasing temperature for both irradiated and unirradiated materials because of increasing hydrogen solubility that leads to more hydrogen in solid solution and less hydride being formed at the crack tip." [33]. Below is shown the cracking velocity data for different temperatures:

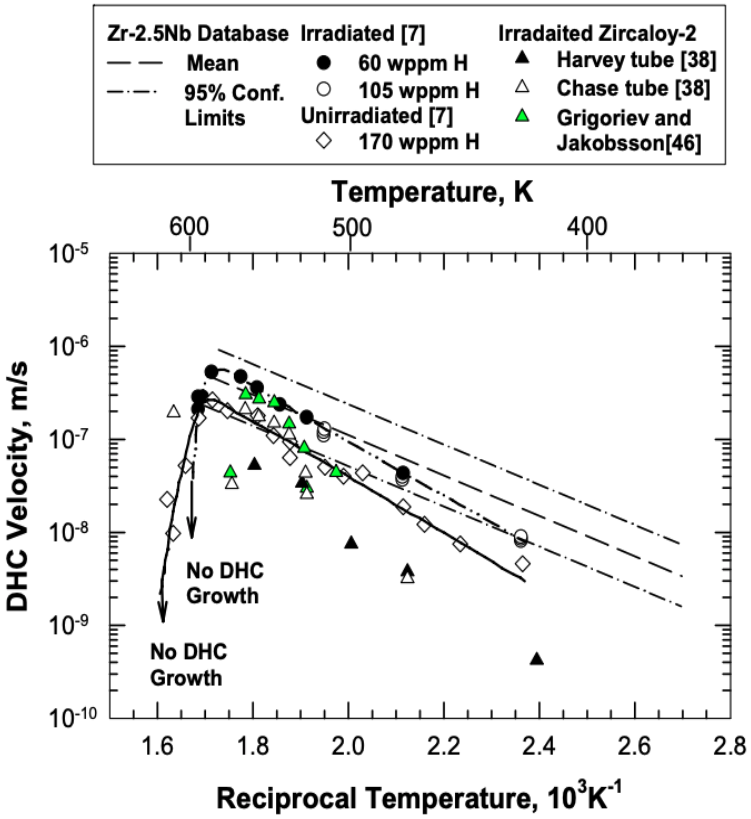

Figure 2.2 - High temperature crack velocity data for DHC in irradiated and unirradiated Zr-2.5 % Nb material. [34]

Chapter 4

In-Reactor and Fuel Pools Safety Criteria

Following the main fuel safety criteria for LWR and Gas Cooled Reactors (GCR) are presented. The structure of this chapter is based on a 2012 OECD's Nuclear Energy Agency technical review of the criteria [35] and a 2006 National Research Council public report on spent nuclear fuel storage [36] for fuel pool safety references. Most of the current fuel safety criteria were established during the 1960s and early 1970s and were based on a conservative approach to regulation.

4.1 In-reactor criteria

4.1.1 Critical Heat Flux

Critical Heat Flux (CHF) describes a thermal limit where a phase change in the reactor coolant occurs during heating. In PWR for example CHF occurs when the bubble density from nucleate boiling near the cladding boundary layer is big enough that a vapour film forms on the surface of the rod inducing rapid oxidation, poor heat tranfert properties of the surroundings of the cladding and subsequent cladding failure. This criteria is inherent to water cooled reactors and has no use in gas cooled systems.

4.1.2 Criticality and shutdown margin

Reactor (or system) subcriticality must be assured either by mechanical neutron absorers (such as control rods) or by sufficient boron concentration in the enviroment where fuel assemblies are kept (liquid or gaseous coolant). An interesting alternative concept is the use of a gaseous control system for GCR using either ^{3}He or boron hydride as gaseous neutron absorbers [37][38].

4.1.3 Stress, strain, fatigue

Stress/strain limits for fuel assemblies are based on specific fuel bundles design and the tested by the fuel vendor to demonstrate the security of the system. The NRC gives more specific information on fuel damage criteria on normal operating conditions and AOOs in NUREG-0800 [39]. It states that fuel safety criteria "should assure that fuel system dimensions remain within operational tolerances and that functional capabilities are not reduced below those assumed in the safety analysis". In particular under SRP Acceptance Criteria 1.A:

i) Stress, strain, or loading limits for spacer grids, guide tubes, thimbles, fuel rods, control rods, channel boxes, and other fuel system structural members should be provided. Stress limits that are obtained by methods similar to those given in Section III of the Boiler and Pressure Vessel Code of the American Society of Mechanical Engineers (ASME) are acceptable. Other proposed limits must be justified.

ii) The cumulative number of strain fatigue cycles on the structural members mentioned in item (i) above should be significantly less than the design fatigue lifetime, which is based on appropriate data and includes a safety factor of 2 on stress amplitude or a safety factor of 20 on the number of cycles. Other proposed limits must be justified.

iii) Fretting wear at contact points on the structural members mentioned in item (i) above should be limited. Fretting wear tests and analyses that demonstrate compliance with this design basis should account for grid spacer spring relaxation. The allowable fretting wear should be stated in the safety analysis report, and the stress and fatigue limits in items (i) and (ii) above should presume the existence of this wear.

4.1.4 PCMI

PCMI is a stress configuration on both cladding and pellets caused by expanding pellets. If the stress is large enough it can result in cladding failure. PCMI-stress-caused cladding failures should be avoided by general cladding stress/strain limits. Generally cladding failures by PCMI is regarded as a secondary risk compared to other mechanisms even though it should be investigated in more detail for high burnup fuel bundles. [35]

4.1.5 Fuel and cladding melting

The melting temperature of UO_2 fuel pellets is around 2865 °C. Zircalloy cladding melting temperature ranges between 1727 °C and 1977 °C and depends on the specific alloy composition and oxygen content [40]. Given the lower melting temperature for the cladding the fuel rod melting phenomena depends mainly on molten zircalloy-pellet interaction and has been studied thoroughly during the years. Of particular importance is the early temperature history of the melting process: we distinguish fast temperature transients and slow temperature transients.

Fast transients ($>$ 0.3 to 0.5 °C/s). In this scenario the cladding melts and drains in a short period of time preventing the dissolution of ceramic UO2 (and subsequent fission products release). [40]

Slow transients ($<$ 0.3 to 0.5 °C/s). In this scenario (with water as coolant) the relocation of molten zircalloy is stopped by the formation of an outer layer of zirconium oxide (ZrO_2). Between the ZrO_2 layer and the pellets the molten zirconium (partially) dissolves UO_2 generating U-O-Zr mixtures. This mixtures stay in place until the failure of the ZrO_2 layer at around 2030 °C. The percentage of fuel pellets dissolution depends on the thickness of the ZrO_2 layer and the concentration of Zr in the molten phase. [40]

4.1.6 LOCA/non-LOCA cladding embrittlement and temperature

According to US NRC regulations the cladding maximum allowable temperature for non-LOCA conditions is 1482 °C (2700 °F). For LOCA conditions the cladding maximum allowable temperature is 1204 °C (2200 °F) [41]. The reason why the temperature limit in LOCA conditions is set to be lower than the temperature limit in non-LOCA conditions is because

in the latter incident transient occur much faster and do not pose a danger to the integrity of the fuel rods [35]. The maximum allowable cladding temperature is chosen as a parameter because it is correlated to the amount of cladding that undergoes oxidation and subsequent embrittlement accident conditions. Note that this limits are set as a result of observation and experiments conducted on low burnup or non-irradiated fuel rods and the validity in regard of high burnup fuel assemblies behaviour is not taken into consideration.

4.1.7 Seismic loads

Dynamic, structural loads arasing from seismic phenomena is often assessed with stresses deriving from high pressure LOCA accident conditions. Most countries do not require specific quantitative design criteria but impose that core coolability and rod insertability must be preserved in combined LOCA and seismic conditions. Such qualitative regulations [42] are similar to:

- fuel rod fragmentation shall not occur;
- control rod insertion shall not be impaired;
- limit spacer distortion to ensure rod coolability.

4.2 Fuel pools criteria

The main objective for spent fuel pools is to keep the temperature of the fuel assemblies as low as possible until the decay heat production decreases significantly with time. The main safety operational concernes for spent fuel pools are therefore:

1. the water and fuel rods temperature should be kept below 50/60°C [43][44];
2. subcriticality should be mantained (via borated water and solid grids separating the assemblies);
3. water chemistry should be tightly controlled to avoid dispersion of radionuclides [45].

It is important to note that different pool technologies are used for spent fuel assemblies generated by different types of reactors (i.e. PWR, BWR, PHWR, GCR...)[45] but the safety principles applied are basically the same.

Part III

Proposed system

Chapter 5

Description

The proposed system is a gas cooled loop that must meet both radiological, thermodynamic and economic constrains. It is based on multiple layers of protection that aim to achieve the complete isolation of radiotoxic elements from the enviroment and expecially the district heating water loop. The main components of the system are:

- **Coffin**: it is a simple pressurized cask containg multiple assemblies. It is filled with an inert gas (helium or nitrogen) to mantain a chemically stable and non corrosive atmosphere.
- **Coolant loop**: an inert gas is chosen as a coolant (but liquid coolants should be evaluated too). The gas picks up heat from multiple coffins through forced convection and releases it to the water via a heat exchanger.
- **Loading mechanism**: different layouts for the whole system are explored in order to achieve a viable strategy for online "refuelling".

Different configurations can be explored including various layouts, materials and thermodynamic parameters. However the system must be complacent with the following criteria:

1. to achieve a meaningful output of district heating water;
2. to remain below accident temperature margins via completely passive natural circulation phenomena in case of complete loss of on site power;
3. to obtain continuous operation through online "refuelling";
4. to be economically feasible.

5.1 Coffin

The coffin is a simple metallic cask containg 4 assemblies. It serves multiple functions:

1. it poses a **barrier** between the assemblies and the cooling gas that will eventually exchange heat with the water. In case of cladding rupture and subsequent fission products release it has to contain safetly all the hazardous materials. In case of major LOCA and eventually a flooding Fukushima-like accident it has to mantain the inert atmosphere and achieve complete separation of water or air moisture and the assemblies.

2. it ensures **subcriticality** of the assemblies.

Following are some pictures of a possible design:

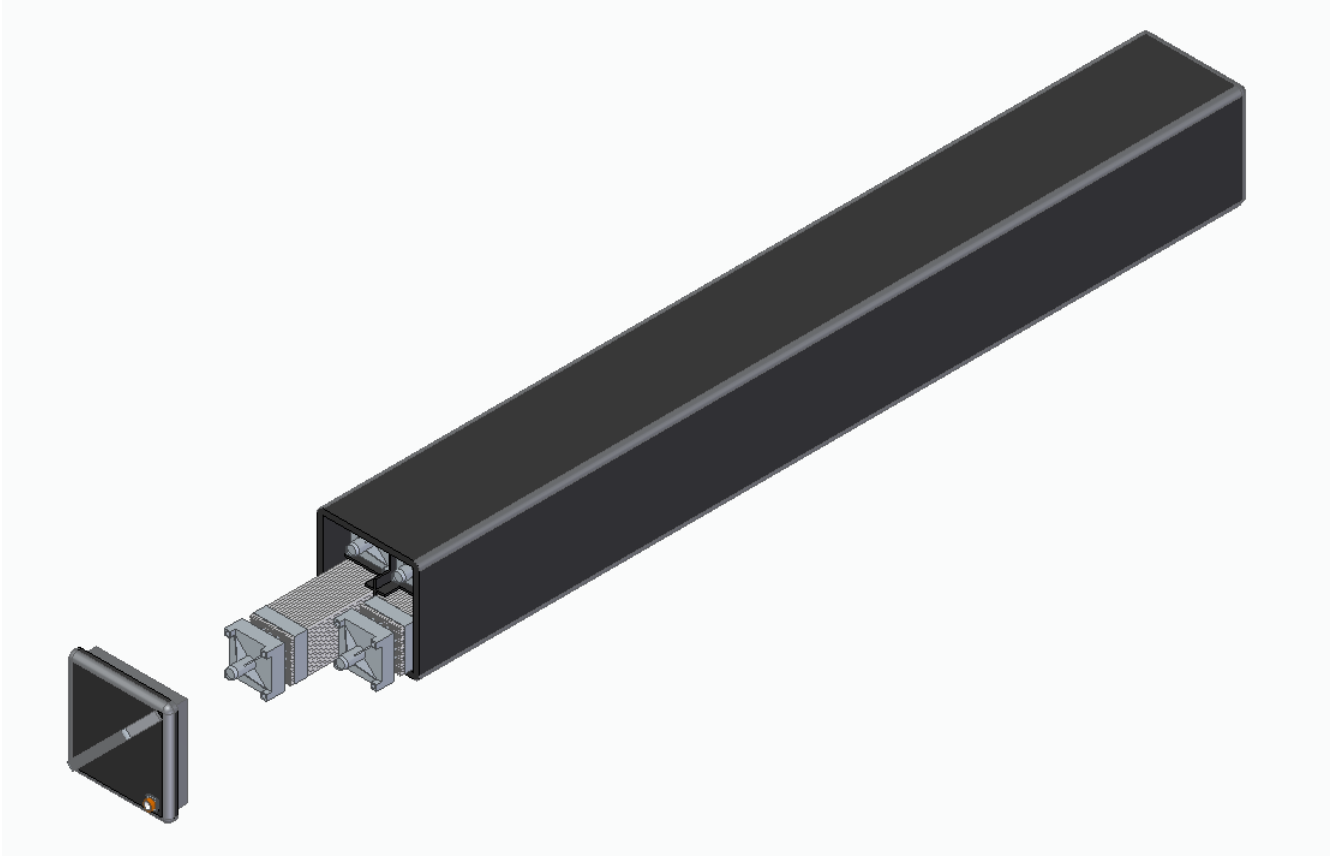

Figure 5.1 - Loading of 4 assemblies on the coffin.

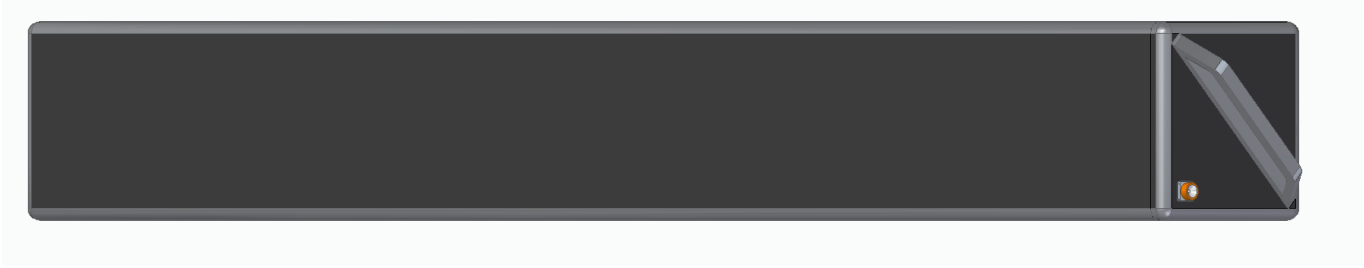

Figure 5.2 - Loaded and enclosed coffin.

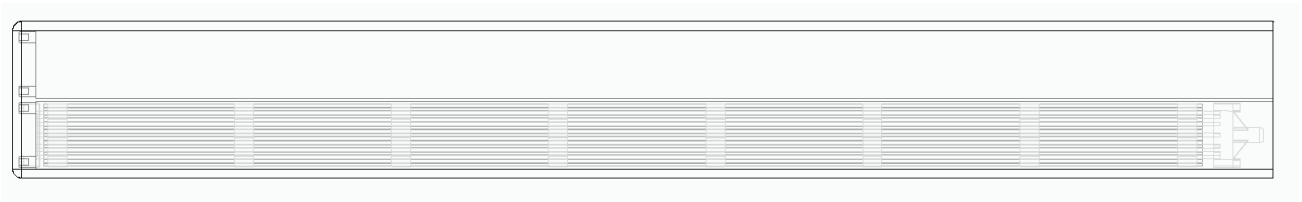

Figure 5.3 - Wireframe view of open coffin with one assembly loaded.

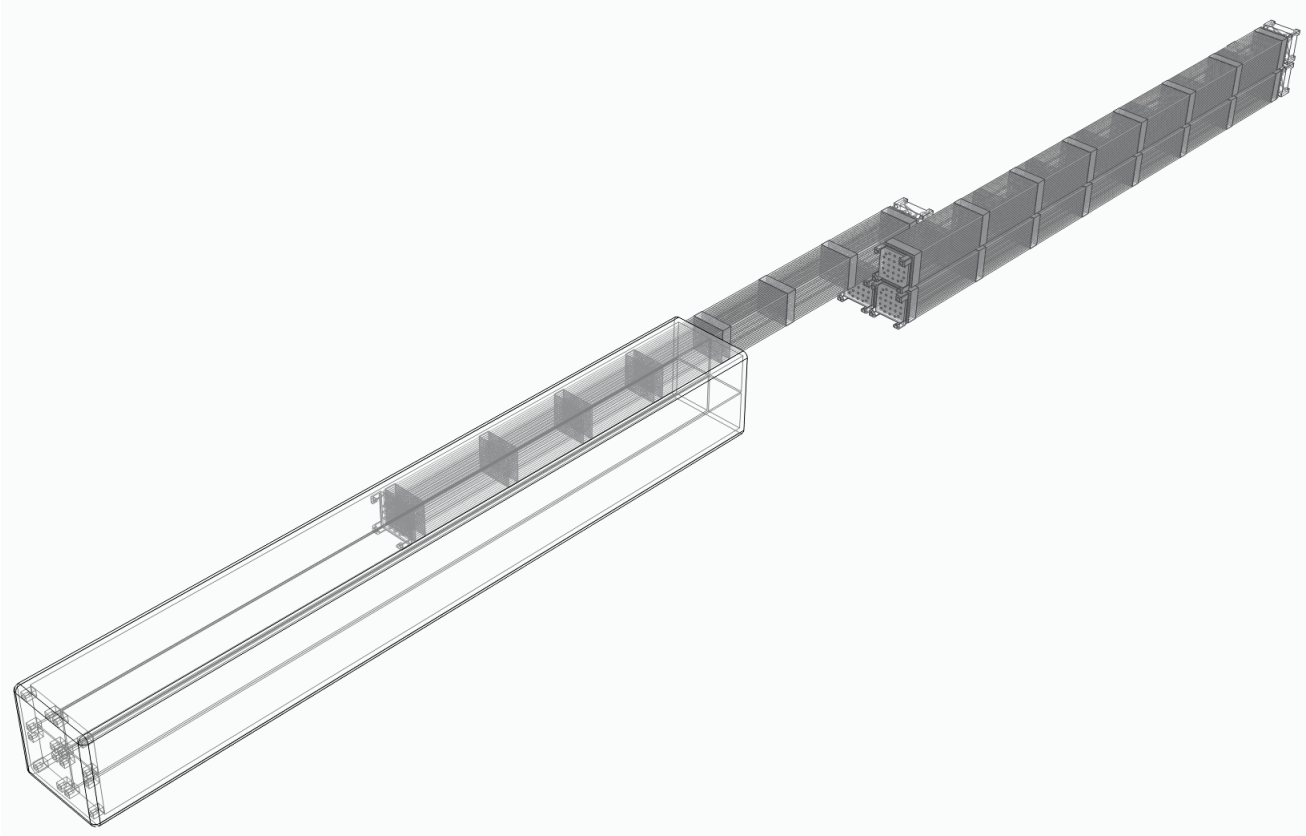

Figure 5.4 - Wireframe view of loading of 4 assemblies.

5.1.1 Shape

There are different shapes we can consider, the ultimate choice depends on the overall layout of the plant. Both squared base prismatic shapes and cylindrical shapes can be implemented. Elements to maximize convective heat transfert should be added (not modeled yet).

5.1.2 Material

The material must be cheap, thermally conductive, pressure and temperature resistant. It also shouldn't be supsceptible to significant radiation-induced damage and neutron activation. Both steel and copper are strong candidates with the latter being very expensive.

5.2 Layout

Various layouts are viable options both for coolant flow and refuelling strategy.

5.2.1 Coolant flow

The coolant flow layout must ensure the efficient heat transfert from the coffins to the coolant and make a natural circulation flow possible. The following are considered:

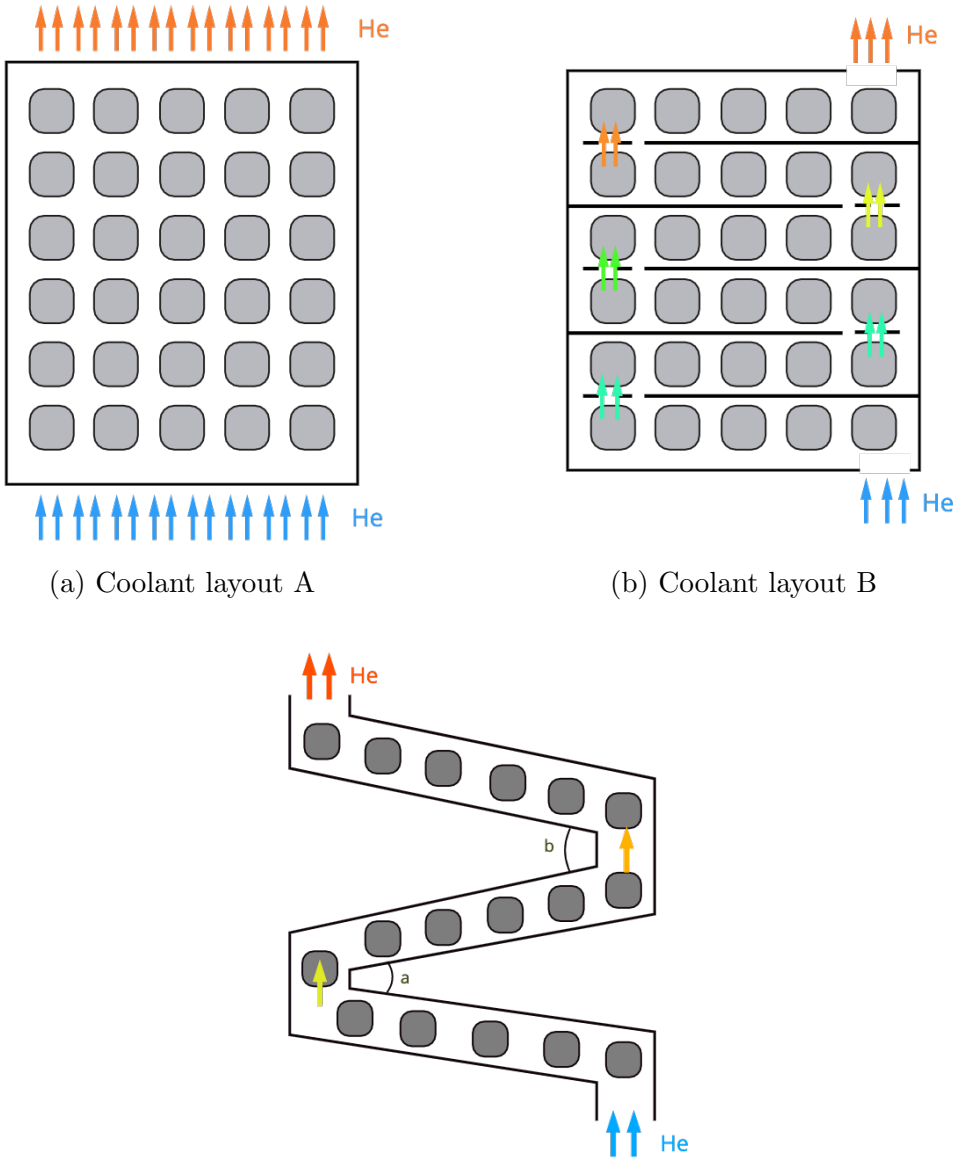

(a) Coolant layout A

(b) Coolant layout B

(c) Coolant layout C

Figure 5.5 - Coolant flow layouts

5.2.2 Refuelling strategy

Online insertion and substitution of loaded coffins must be achieved. The only way to make this possible is to use an intermidate pressurization chamber. The following layouts are considered:

- axially-aligned axial loading;
- axially-aligned top loading;
- horizontally-aligned lateral loading;

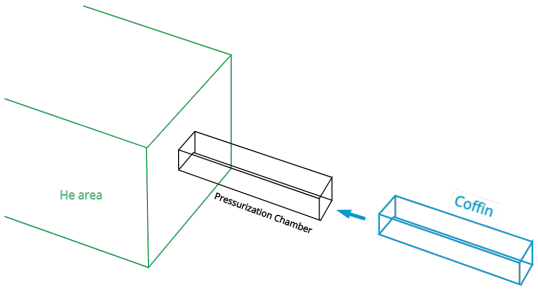

(a) Axially-aligned axial loading

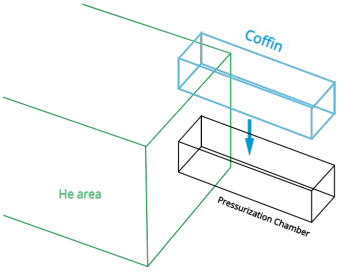

(b) Axially-aligned top loading

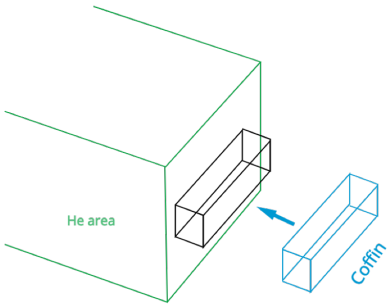

(c) Horizontally-aligned lateral loading

Figure 5.6 - Refuelling layouts

Here are some advantages and disadvantages of the strategies:

(a) Axially-aligned axial loading. The main advantage is the easy engineering of the pressurization chamber since only the bottom and top of the prism are mobile. The design is nevertheless very space-inefficient because of the height of the assemblies and coffin. This configuration makes it impossible to place the system underground while mantaining viable economics.

(b) Axially-aligned top loading. This strategy is very challenging from a pressurization chamber engineerng point of view. In order to make all the levels of the system accessible the only possible configuration is to build one row of pressurization chambers and make it vertically mobile. It is also quite space-inefficient.

(c) Horizontally-aligned lateral loading. This is the only viable strategy since the configuration is compact enough. The main hurdle is the engineering of the lateral opening of the pressurization chambers but since the system is not meant to operate at very high pressures this should be viable.

5.2.3 System layout

Having identified just one viable refuelling strategy we can combine the coolant layouts and the refuelling system. The pressurization chambers are added to both coolant layout B and C.

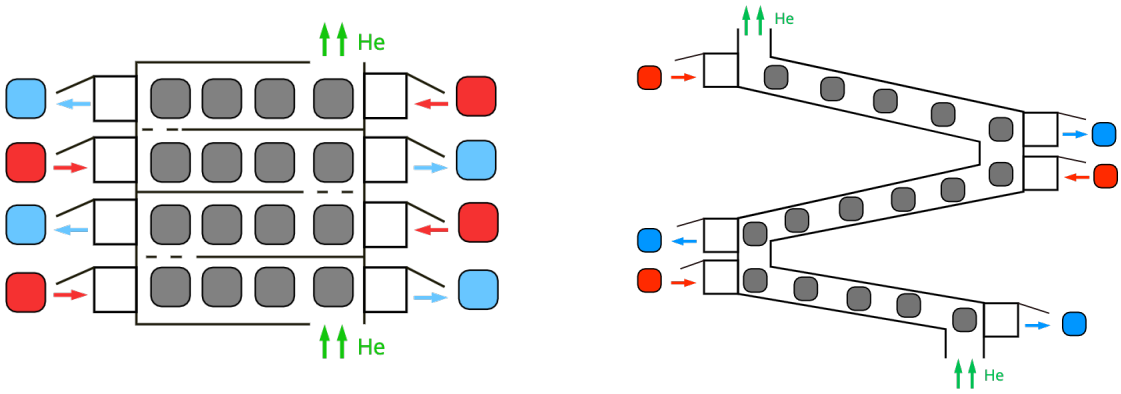

(a) Complete configuration B

(b) Complete configuration C

Figure 5.7 - Complete configurations (coolant layouts with pressurization chambers)

Both configurations make it possible to quickly insert and remove coffins while mantaining the system up and running.

Bibliography

[1] WORLD NUCLEAR ASSOCIATION, Nuclear Fuel and its Fabrication (updated 2020)

[2] Ade, Brian and Gauld, Ian (2011). Decay Heat Calculations for PWR and BWR Assemblies Fueled with Uranium and Plutonium Mixed Oxide Fuel using SCALE.

[3] Measurements of decay heat in spent nuclear fuel at the Swedish interim storage facility (Part 1), Clab. SKB Rapport R-05-62. ISSN 1402-3091

[4] SCALE: A Modular Code System for Performing Standardized Computer Analyses for Licensing Evaluation. Version 5, ORNL/TM-2005/39, I-III, ORNL (2005).

[5] W.B. Waihermiller and G. S. Allison, 1979, LWR NUCLEAR FUEL BUNDLE DATA FOR USE IN FUEL BUNDLE HANDLING (pages 8,15). PNL-2575.

[6] US DOE, osti 5202618, Characteristics of spent fuel, high-level waste, and other radioactive wastes which may require long-term isolation, December 1987.

[7] Osti 6234717. Hermann, O W and Alexander, C W, Review of spent-fuel photon and neutron source spectra, January 1986.

[8] Lee, Se Geun and Cheong, Jae Hak, Neutron Activation of Structural Materials of a Dry Storage System for Spent Nuclear Fuel and Implications for Radioactive Waste Management, Energies, volume 13, 2020, article number 5325, ISSN 1996-1073.

[9] NRC (U.S. Nuclear Regulatory Commission, 2008). Title 10, Code of Federal Regulations, Part 72, "Energy: Licensing Requirements for the Independent Storage of Spent Nuclear Fuel and High-Level Radioactive Waste, and Reactor-Related Greater than Class C Waste," Washington, DC: Office of Federal Register National Archives and Records Administration, U.S. Government Printing Office, as amended June 9, 2008 (10 CFR 72).

[10] NRC (U.S. Nuclear Regulatory Commission) Spent Fuel Project Office Interim Staff Guidance - 11, Revision 3

[11] United States Nuclear Waste Technical Review Board. "Evaluation of the Technical Basis for Extended Dry Storage and Transportation of Used Nuclear Fuel", 2010, (page 28).

[12] "Spent Fuel Transportation Applications -Assessment of Cladding Performance A Synthesis Report",EPRI, Palo Alto, CA: 2007. 1015048.

[13] "Creep as the Limiting Mechanism for Spent Fuel Dry Storage," EPRI, Palo Alto, CA: 2000. 1001207.

[14] David J. Richmond, Kenneth J. Geelhood, FRAPCON analysis of cladding performance during dry storage operations, Nuclear Engineering and Technology, Volume 50, Issue 2, 2018, Pages 306-312, ISSN 1738-573.

[15] Elmar Eidelpes and Luis F. Ibarra and Ricardo A. Medina, Probabilistic Assessment of Peak Cladding Hoop Stress and Hydrogen Content of PWR SNF Rod Cladding, Nuclear Technology, Volume 205, Issue 8, 2019, Pages 1095-1118, Taylor and Francis.

[16] "Step 4: Assessment of Spent Fuel Interim Storage for the UK Advanced Boiling Water Reactor", Office for Nuclear Regulation (ONR), Assessment Report ONR-NR-AR-17-030, Revision 0, 2017.

[17] Kyu-Tae Kim, The effect of peak cladding temperature occurring during interim-dry storage on transport-induced cladding embrittlement, Nuclear Engineering and Technology, Volume 52, Issue 7, 2020, Pages 1486-1494, ISSN 1738-5733.

[18] Ki-Nam Jang, Hyun-Jin Cha, Kyu-Tae Kim, Allowable peak heat-up cladding temperature for spent fuel integrity during interim-dry storage, Nuclear Engineering and Technology, Volume 49, Issue 8, 2017, Pages 1740-1747, SSN 1738-5733.

[19] K. Kimura Integrity criteria of spent fuel for dry storage in Japan International Seminar on Spent Fuel Storage(ISSF), Tokyo, Japan (2010).

[20] NRC Amendement A1 – ML20136A051, Final Tech Specs - EOS AMD 1

[21] NRC Amendement A4 – ML19036A558, Technical Specifications [Letter to P. Narayanan re: Amendment No. 4 to Certificate of Compliance No. 1029 for the Standardized Advanced NUHOMS System]

[22] NRC Amendement A1 - ML073050262, Enc. 1A (Tech Specs) Certificate of Compliance No. 1027 for the TN-68 Dry Storage Cask.

[23] NRC Amendement A8 - ML19038A251, Enclosure 2: TS Appendix A and B, Amendment No. 8 [Letter to W. Fowler re: Amendment Nos. 7 and 8 to Certificate of Compliance No. 1025 for the NAC-Multi Purpose Canister Storage System]

[24] ASTM C 1553 – 2008, "Standard Guide for Drying Behavior of Spent Nuclear Fuel," ASTM International, pp. 1-16.

[25] Jung H., Shukla P., Ahn T., Tipton L., Das K., He X., Basu D. - US NRC Contract NRC–02–07–006, 2013

[26] B.D. Hanson, R.D. Daniel, A.M.Casella, R.S. Wittman, W. Wu, P.J. MacFarlan, and R.W. Shimskey (2008). "Fuel-In-Air FY07 Summary Report," Pacific Northwest National Laboratory for DOE, PNNL-17275, Rev. 1

[27] Hanson B.,Revision 00 of ANL-EBS-MD-000013, "Clad Degradation- Dry Unzipping"

[28] Hanson B.,Revision 00 of ANL-EBS-MD-000013, "Clad Degradation- Dry Unzipping", table 9 (pag. 38) and table 12 (pag. 45)

[29] R.E. Einziger, H. Tsai, and M.C. Billone (2003). "Examination of Spent Pressurized Water Reactor Fuel Rods After 15 Years in Dry Storage," Nuclear Technology, Vol. 144, pp. 191-92.

[30] C.K. Chao, K.C. Yang, C.C. Tseng (2008). "Rupture of Spent Fuel Zircaloy Cladding in Dry Storage Due to Delayed Hydride Cracking." Nuclear Engineering and Design, 238: 1, January 2008, p. 125.

[31] Masami MAYUZUMI , Takeo ONCHI and Yutaka MATSUO (1993) Failure Propensities of Pressurized Zircaloy Tube Containing Iodine and Other Chemical Species, Journal of Nuclear Science and Technology, 30:12, 1288-1298

[32] Manfred P. Puls, The effect of Hydrogen and Hydrides on the Integrity of Zirconium Alloy Components - Delayed Hydride Cracking, Springer, 2012, ISBN 978-1-4471-4194-5

[33] Kwai S. Chan (2013), "An Assessment of Delayed Hydride Cracking in Zirconium Alloy Cladding Tubes Under Stress Transients", Southwest Research Institute.

[34] Kwai S. Chan (2013), "An Assessment of Delayed Hydride Cracking in Zirconium Alloy Cladding Tubes Under Stress Transients", Southwest Research Institute, (figure 14).

[35] Nuclear Fuel Safety Criteria Technical Review (Second Edition), 2012, OECD Nuclear Energy Agency. NEA No. 7072. ISBN 978-92-64-99178-1

[36] National Research Council, Safety and Security of Commercial Spent Nuclear Fuel Storage: Public Report, 2006, ISBN 978-0-309-09647-8

[37] Abdel-Khalik, 1991. Gaseous Reactor Control System. US Patent 5045275.

[38] S.A. Hosseini, Neutronic analysis of a gaseous control system for the HTR-10 reactor, Annals of Nuclear Energy, Volume 45, 2012, Pages 80-85, ISSN 0306-4549

[39] NRC NUREG-0800 - Chapter 4, Section 4.2, Revision 3, Fuel System Design (SRP acceptance criteria)

[40] Chapter 2 - In-Vessel Core Degradation, Editor(s): Bal Raj Sehgal, Nuclear Safety in Light Water Reactors, Academic Press, 2012, Pages 89-183, ISBN 9780123884466.

[41] US NRC 10CFR50.46

[42] US NRC, NUREG-0800, SRP 4.2, App. A

[43] Westinghouse Technology Systems Manual Section 14.4 Spent Fuel Pool Cooling and Cleanup System

[44] A. B. Johnson Jr., Behaviour of spent nuclear fuel in water pool storage, 1977, Pacific Northwest Laboratories, BNWL-2256.

[45] Storage of water reactor spent fuel in water pools, IAEA, 1982.